RSC Advances

ROYAL SOCIETY OF CHEMISTRY

www.rsc.org/advances

RSC Advances

RSCPublishing

ARTICLE

Anisotropic hierarchical porous hydrogels with unique water losing/absorbing and mechanical properties

Cite this: DOI: 10.1039/x0xx00000x

Di Zhao, Jintang Zhu, Zhongcheng Zhu, Guoshan Song and Huiliang Wang*

Received 00th April 2014,
Accepted 00th April 2014

DOI: 10.1039/x0xx00000x

www.rsc.org/

Hydrogels with aligned porous structures have many potential applications. Introducing hierarchical porous structures into hydrogels might impart them with more and better functionalities. In this work, we prepared poly(2-hydroxyethyl methacrylate-*co*-acrylamide) [P(HEMA-*co*-AAm)] hydrogels with directional freezing redox polymerization method by varying the molar ratio of HEMA to AAm. The P(HEMA-*co*-AAm) hydrogels have anisotropic hierarchical porous microstructures, *i.e.* large-area, thick lamellar structures aligned along the freezing direction are connected with thin lamellar bridges, forming macro-pores (several tens to more than 100 μm), and the large lamellar structures change from dense to be with many micro-pores. The large and long aligned channels provide the path for the unidirectional diffusion of solutions. The hierarchical porous structure and the hydrophilic nature of AAm lead to enhanced equilibrium water contents of the hydrogels, which can reach 95%. The hydrogels lose water under compression, the ratio of water that can be squeezed out reaches 66.7% of the total water content, and the squeezed gels can absorb water very quickly when swollen in water again. The hydrogels show anisotropic mechanical properties, with better tensile and compressive properties in the parallel direction. Interestingly, for the hydrogels synthesized with higher AAm molar ratios, their tensile stress-strain curves are almost linear. In addition, the hydrogels also exhibit perfect elastic recovery performance.

Introduction

Normal synthetic hydrogels are generally isotropic in both microstructures and properties. Whereas biological gels, which are the main components of animal tissues, usually have anisotropic microstructures and properties.[1-3] For example, jellyfish mesogloea has a well-developed anisotropic microstructure, which is consisted of aligned nano-sized membranes and nano-fibers connected with them.[4, 5] The jellyfish mesogloea also exhibits very interesting and unique anisotropic swelling properties.[4] Anisotropic hydrogels especially those with aligned porous structures have drawn much attention,[6, 7] due to their great potential applications as catalyst carriers,[8-10] substrates for cell culture,[11-13] and bioscaffolds.[14-16]

Directional freezing (DF) is a very simple, environmentally friendly and cost-effective physical method for fabricating inorganic, polymeric materials and polymer composites with aligned porous structures.[17-23] Several hydrogels have also been fabricated with the DF method. Unfortunately, the application of DF method in hydrogel preparation is strongly impeded by the quite limited number of raw materials, since only those polymers which can form strong hydrogen bonding can be used. Polyvinyl alcohol (PVA) is the most commonly used synthetic polymer.[24-26] More commonly employed polymers are natural polymers, such as agar,[27] agarose,[28] chitosan and alginate,[29-31] collagen,[32] gelatin,[33] proteins,[34] *etc*. The hydrogels made with as-prepared or naturally occurring polymers are usually unstable at a high temperature due to the breakage of hydrogen bonding, unless extra chemical bonding is introduced among the polymer chains by further chemical cross-linking reactions.

Starting from monomers is a better and more versatile choice, since there are many hydrophilic monomers can be used for hydrogel preparations and physical/chemical cross-links can be introduced during the polymerization process. Therefore, the combination of directional freezing and polymerization (DFP) in the frozen state provides a method for making gels with aligned porous structure. Dogu and Okay prepared butyl rubber organogels with aligned macroporous structures by applying DFP method.[35] Very recently, Zhang's group[36, 37] and Okaji *et al.*[38] reported the fabrication of hydrogels with directional freezing and photo polymerization method. Our group has also reported the fabrication of anisotropic poly(2-hydroxyethyl methacrylate) (PHEMA) hydrogels by combining directional

freezing method and γ-rays radiation-induced polymerization and crosslinking method (DFRPC)[39] or redox polymerization method (DFRP).[40] These hydrogels have aligned channels in the direction parallel to the freezing direction. The anisotropic porous structures of the gels impart them with anisotropic mechanical properties. The PHEMA hydrogels show high tensile and compressive strengths, as well as high fracture energies, and the mechanical properties are usually better in the direction parallel to the freezing direction.[39, 40]

The hydrogels made with the DFP method usually have dense channel walls, as the phase separation during the DF process leads to the aggregation of monomer molecules which subsequently polymerize at a low temperature to form a dense polymer phase. The strong chemical and/or physical interactions among the polymer chains lead to the good mechanical properties of the hydrogels. However, as the disadvantageous side, the dense channel walls lead to poor interconnectivity through the micro-tube walls, which are unfavourable for the application of gels as a catalyst carrier or a bio-scaffold.[41]

Introducing porous structures onto the dense channel walls, *i.e.* forming hierarchical porous structures, might impart the hydrogels with more and better functionalities. The microstructure of a material prepared with the DF method is strongly depended on the phase separation in the freezing process.[42, 43] Using mixed solvents or monomers with different freezing points and solubility may cause different phase separation in the freezing process, and hence obtain hydrogels with hierarchical porous structures.

In this work, we employed directional freezing redox polymerization method to prepare hydrogels, using HEMA and AAm as the monomers. By varying the molar ratios of HEMA to AAm, poly(2-hydroxyethyl methacrylate-*co*-acrylamide) [P(HEMA-*co*-AAm)] hydrogels with hierarchical porous structures and unique water losing/absorbing and mechanical properties were obtained.

Experimental

Materials

2-Hydroxyethyl methacrylate (HEMA, 98.0%) was purchased from Aladdin Reagent Database Inc. (Shanghai, China), ultra-pure grade acrylamide (AAm) was from ZhongBei LinGe Biotechnology Ltd. (Beijing, China), *N, N, N′, N′*-tetramethylethylenediamine (TEMED, 99.0%) was from Beijing InnoChem Science & Technology Co. Ltd. (Beijing, China), and potassium persulfate (KPS) was purchased from Shanghai Chemical Reagent Company (Shanghai, China). Deionized water was used for preparations of all aqueous solutions. All of these materials were used without future purification.

Hydrogel preparation

HEMA and AAm monomers were dissolved in water, in which the total concentration of the monomers was 3 mol L^{-1} and the molar ratios of HEMA to AAm were 5:1, 2:1, 1:1, 1:2 and 1:5, respectively. KPS and TEMED were used as the redox initiator system, and the molar ratio of monomer/KPS/TEMED was 100/1/1.

To fabricate the hydrogels, firstly, the solution (without redox agent) was injected into a test tube or a tubular mould and then was bubbled with nitrogen gas for 5 min in an ice-water bath. After the addition of initiators, the test tube or the tubular mould was placed in directional freezing equipment to perform the unidirectional freezing at the freezing rate of 2 mm min^{-1} until the whole solution was frozen. Subsequently, the frozen sample was put into a fridge (-20 ℃) for 48 h to ensure the completion of the redox polymerization. Finally, the sample was thawed at room temperature, and then it was washed by deionized water to remove the unreacted reactants and the oligomers. The hydrogel samples were swollen in deionized water to equilibrium swelling for future use.

Scanning electron microscopy (SEM) investigations

The P(HEMA-*co*-AAm) hydrogels were cut into strips and then plunged into liquid nitrogen for about 5 min. The frozen strips were subsequently freeze-dried in the FD-1B-50 vacuum freeze dryer (Beijing Boyikang Laboratory Apparatus Co., Ltd.) for 48 h until all water was removed. The dried samples were cracked in the directions vertical and parallel to freezing direction. After being sputter-coated with gold for 15 min, the morphologies of these fractured surfaces were observed with a Hitachi S-4800 cold field emission scanning electron microscope (Tokyo, Japan) with an accelerating voltage of 5 kV.

Water content measurements

The equilibrium swollen P(HEMA-*co*-AAm) hydrogels were cut into cylindrical shaped specimens and weighed after the surface water was removed by wiping with filter paper, then the weighed hydrogels were vacuum dried at 60 ℃ for 24 h. The equilibrium water content is calculated as EWC= $(m_{wet}-m_{dry})/m_{wet}\times100\%$, where m_{wet} and m_{dry} are the masses of the swollen specimens and the dried samples, respectively.

The P(HEMA-*co*-AAm) hydrogels lose water under an applied stress. To evaluate the change of water content during the compression tests, the masses of the specimens before and after testing were measured. The squeezed out water content was calculated as SWC= $(m_1-m_2)/m_1\times100\%$, where m_1 and m_2 were the masses of the swollen specimens before and after compressed to no more water can be squeezed out.

Mechanical tests

Dumbbell shaped gel specimens standardized as DIN-53504 S2 (overall length: 75 mm; width: 10 mm; inner width: 4 mm, gauge length: 20 mm, thickness: 2 mm) for tensile tests were cut from swollen P(HEMA-*co*-AAm) hydrogels in both directions parallel and vertical to the freezing direction. For compression testing, the hydrogels were cut into cylindrical shaped specimens (10 mm in diameter and about 5 mm in height).

All the tests were performed by using an Instron 3366 electronic universal testing machine (Instron Corporation, MA, USA). 100 N load cell and 400% min^{-1} crosshead speed were applied for tensile tests, and 10 kN load cell and 25% min^{-1} crosshead speed were applied for compression tests, respectively. Five specimens per experimental point were tested to obtain reliable values.

The tensile stress σ_t is calculated as follows: $\sigma_t = Load/tw$ (t and w are the initial thickness and width of the dumbbell shaped gel sample, respectively). The tensile strain ε_t is defined as the change in the length relative to the gauge length of the freestanding specimen. Tensile fracture stress or tensile strength (σ_b) is the tensile stress at which the specimen breaks. The compressive stress σ_c, is calculated by $\sigma_c = Load/\pi r^2$, where r is the original radius of the specimen. The strain (ε_c) under compression is defined as the change in the thickness (h) relative to the original thickness (h_0) of the freestanding specimen. Compressive stress and strain between ε_c =10-30% were used to calculate initial elastic modulus (E_c).

Results and discussion

Hydrogels were synthesized with a fixed total monomer concentration of 3 mol L^{-1} but varying molar ratios of HEMA to AAm. Hereafter, the P(HEMA-*co*-AAm) hydrogels are referred to as Gel-x-y, where x and y express the molar ratios of HEMA and AAm, respectively.

Microstructures

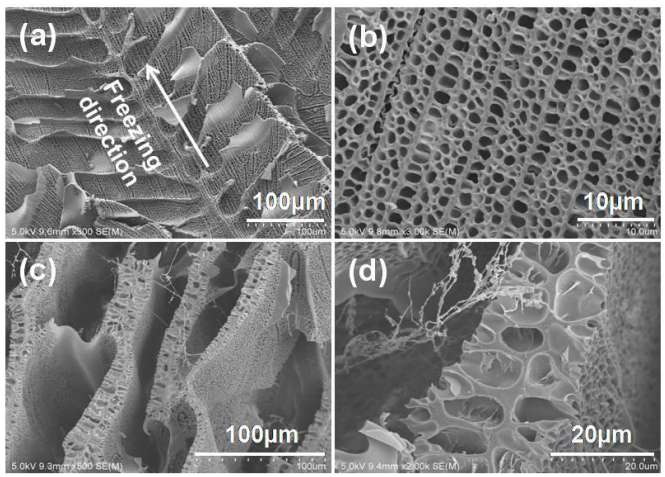

Fig. 1. SEM micrograms of the Gel-1-1 hydrogel fabricated by DFRP in the direction parallel (a, b) and vertical (c, d) to the freezing direction.

The microstructures of the hydrogels were investigated with SEM. Generally, the hydrogels show obvious anisotropic microstructures. Fig. 1 shows the SEM micrograms of the hydrogel synthesized with an equimolar HEMA and AAm (Gel-1-1). In the direction parallel to the freezing direction, there are very large-area lamellae with some dendrite structures on the surface (Fig. 1a), and the lamellae are composed of tiny aligned pores with the size of 0.5-3 μm (Fig. 1b). In the vertical direction, thick lamellae with a thickness of about 20 μm are found and the lamellae are connected by thin lamellar bridges which correspond to the dendrites, the gap between the adjacent lamellae is several tens to more than 100 μm (Fig. 1c). In addition, pores are found on both sides of the lamellae, but they are not interconnected (Fig. 1d).

The microstructures of the of P(HEMA-*co*-AAm) hydrogels synthesized with different molar ratios of HEMA to AAm are shown in Fig. 2. In the parallel direction (Fig. 2a-d), lamellar structures can be found in all samples, and with the decrease of x/y ratio, the lamellae change from dense to porous. More and lager micro-pores appear on the lamellae with the increase of AAm molar ratio, and the size of the micro-pores varies from 1.11 μm for Gel-2-1 to 3.89 μm for Gel-1-5 (Table S1). In the vertical direction (Fig. 2e-h), the thickness of the lamellae become larger, and more and larger pores appear on them. More importantly, the pores become interconnected for the Gel-1-2 (Fig. 2g) and Gel-1-5 (Fig. 2h) with higher AAm molar ratios.

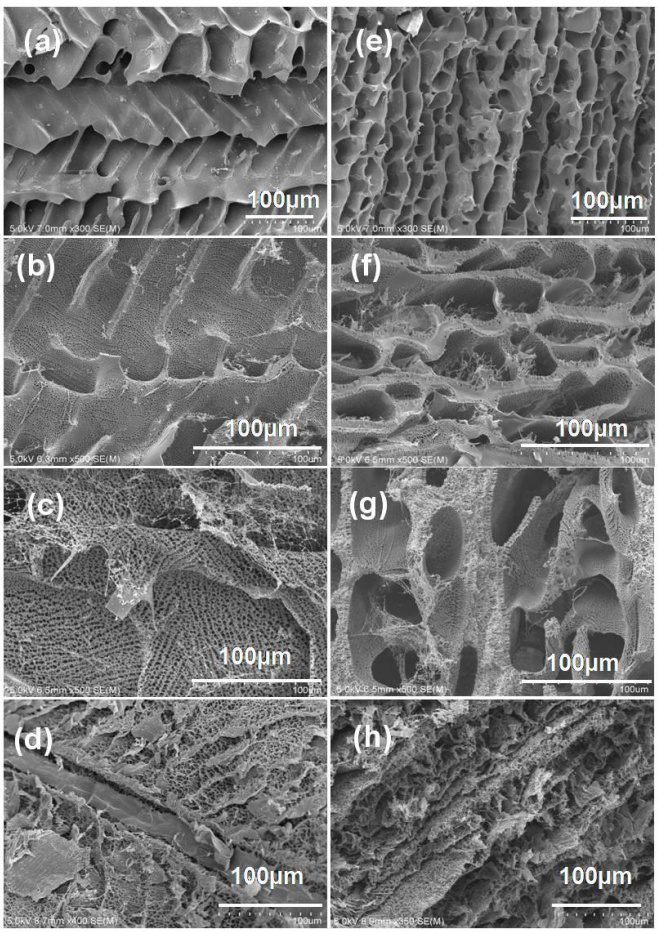

Fig. 2. SEM micrograms of the P(HEMA-*co*-AAm) hydrogels synthesized with different molar ratios of monomers in the parallel direction (a-d) and vertical directions (e-h). (a, e): Gel-5-1, (b, f): Gel-2-1, (c, g): Gel-1-2, and (d, h): Gel-1-5.

The P(HEMA-*co*-AAm) hydrogel have anisotropic microstructures. Compare with the microstructure of PHEMA hydrogels,[39, 40] the introduction of AAm change the dense channel walls to lamellae composed of aligned micro-pores.

These micro-pores on the lamellae and the macro-pores together constitute the hierarchical porous structure. The hierarchical porous structures enhance the interconnection of adjacent holes, and it will be beneficial to some applications of hydrogels, such as catalyst carrier and bio-scaffolds.

The phase separation process of ceramic slurry in the directional freezing has been studied by Deville et al,[42-45] and Barrow *et al*. have also given the similar phase separation process in monomer solutions.[37-40] We believe that in our systems similar phase separation process has occurred. According to the microstructure, the formation mechanism of the P(HEMA-*co*-AAm) hydrogel microstructures can be considered as follows: during the directional process of HEMA and AAm solution, lamellar ice crystals grows unidirectionally from the bottom to the top of the solution, and the monomer molecules and the initiators are separated and aggregated among the gaps between the ice crystals, after polymerization and the removal of ice crystals, lamellar structures with macro-pores in the vertical direction were obtained. As HEMA and AAm have big difference in melting point and solubility, phase separation may happen between these two monomers. More and lager micro-pores are formed on the lamellae with the increase of AAm molar ratio. The possible reason is that more water is bound to the more hydrophilic AAm, and the freezing of bound water occurs at a lower temperature than the free water (Fig. S1), leading to a further phase separation and hence the formation of the micro-pores on the lamellae.

Unidirectional diffusion property

The anisotropic microstructures of the P(HEMA-*co*-AAm) hydrogels lead to their anisotropic properties. The gels exhibit large and long channels aligned along the freezing direction. The large and long aligned channels provide the path for the unidirectional diffusion of solutions. To prove this, we carried out the following experiment: an aqueous solution containing methyl orange was syringed into a swollen cylindrical hydrogel sample along the freezing direction in a short time (< 1 min), and then the sample was immediately cut into two parts, we found that the reddish orange dye diffused mostly along the freezing direction (Fig. 3).

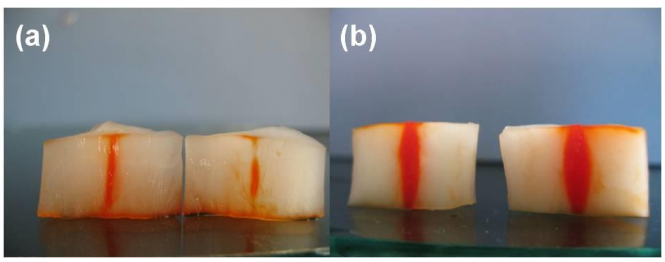

Fig. 3. The diffusion of dye in the equilibrium swollen gels (1 cm thick). (a): Gel-1-1, and (b): Gel-2-1.

Water absorbing and losing properties

The equilibrium swelling water contents (EWCs) and the corresponding equilibrium swelling ratios (ESRs) of the as-prepared P(HEMA-*co*-AAm) hydrogels are shown in Table 1. The EWCs of the gels are generally more than 80%, which is higher than that of PHEMA hydrogel (about 75%) reported previously,[40] and it increases with the molar ratio of AAm to HEMA. When the molar ratio of HEMA to AAm is 1/5, the EWC can reach 95.6%. The increased EWC is due to the introduction of the more hydrophilic monomer AAm and the hierarchical porous structure of the hydrogels.

Table1. Water contents of hydrogels synthesized with different molar ratios.

x/y (mol/mol)	5/1	2/1	1/1	1/2	1/5
EWC (%)	80.4	87.0	89.5	92.4	95.6
ESR[a]	4.10	6.69	8.52	12.2	21.7
ESR[b]	1.13	1.88	3.32	4.74	9.53
SWC (%)	48.7	52.3	55.7	59.9	63.8

[a]: as-prepared hydrogels; [b]: dried hydrogels.

It is necessary to mention that when the as-prepared hydrogels are dried, then they cannot swell to their original sizes. The ESRs of the dried hydrogels (Table 1, and Fig. S1) are lower than those of the as-prepared hydrogels, and the ratio of the two ESRs is more obvious for the hydrogel with a higher HEMA molar ratio. The possible reason is that the close contact of polymer chains in the dried state leads to stronger hydrophobic interactions and hydrogen bonding among them and they cannot be fully broken during the re-swelling process. The following tests were performed on equilibrium swollen as-prepared hydrogel samples.

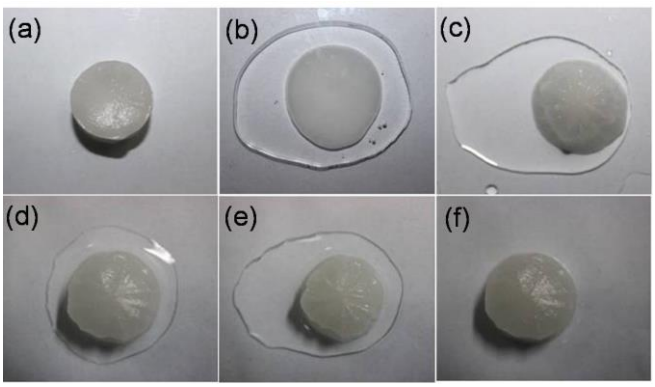

Fig. 4. Photos of the hydrogel before (a) and after (b) being compressed, and (c-f): the process of water-absorbing by the hydrogel after compression.

Due to the presence of large pores in the gels, the water in the swollen hydrogels can be squeezed out easily. Fig. 4a and 4b shows that when a swollen gel was compressed between two glass plates, a lot of water was squeezed out. The contents of water that can be squeezed out (SWC) from the P(HEMA-co-AAm) hydrogels were quantitatively measured (Table 1). With the decrease of the molar ratio of HEMA to AAm (x/y), the SWC of the gels increases. When the value of x/y is 1/5, the

SWC can reach 63.8%, *i.e.* 66.7% of the equilibrium water content can be squeezed out.

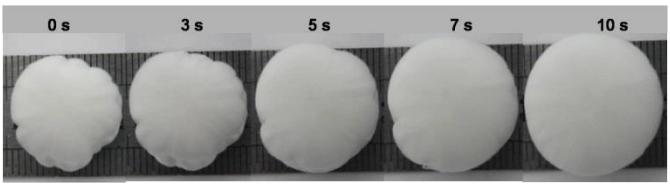

Fig. 5. The change of the shape of a squeezed Gel-1-1 hydrogel sample (1 cm thick) after it was put into water.

The water squeezed out could be completely absorbed by the gel in about two minutes and the gel recovered its original shape simultaneously (Fig. 4c-4e, and Supporting Movie S1). If the squeezed hydrogel was put into a large excess of water, it recovered more quickly. Fig. 5 shows the change of the shape of a squeezed Gel-1-1 hydrogel sample (1 cm thick) after it was put into water. The squeezed hydrogel sample showed an irregular shape, but when it was immersed into water it recovered to its original round shape in only about 10 s (Supporting Movie S2). The water losing property under compression and the fast water absorbing property of the P(HEMA-*co*-AAm) hydrogels are attributed to their elastic macroporous structures.

The gels behave like sponges. We think that the sponge-like hydrogels may find some potential applications as adsorbents and separating materials. This will be studied in our future work.

Mechanical properties

The P(HEMA-co-AAm) hydrogels could be compressed to very high strains without breakage. Fig. 6a and 6b show the elastic moduli (E_c) and compression strengths (σ_c, at ε_c=90%) of the hydrogels in the direction parallel (p) and vertical (v) to the freezing direction, respectively. It is obvious that these gels show anisotropic mechanical properties, as the E_c and σ_c in the parallel direction are generally higher than those in the vertical direction. The anisotropic mechanical properties should result from the anisotropic microstructure of the hydrogels. The higher E_c and σ_c in the parallel direction is due to the stronger chemical and physical interactions in the large-area, continuous and thicker lamellae with comparison to the thin lamellar bridges (dendrites) in the vertical direction (Figs. 1 and 2).

With the increase of AAm molar ratio, E_c and σ_c in both directions decrease. One obvious reason is the increase of the water content of gels with the increase of AAm molar ratio. The other one is the change of the porous structure, the dense channel walls change to porous structures with more and larger pores, which are more effective in distributing applied load and hence lead to the decrease of E_c and σ_c.

It is worthy of noting that biggest difference in the ratio of E_c in the parallel direction to that in the vertical direction is found at the molar ratio of 1/1 (Fig. S3). The possible reason is that the ratio of the thickness of the lamellae in the parallel direction to that in the vertical direction is higher at the molar ratio of 1/1 (Fig. 1) than those at other molar ratios (Fig. 2).

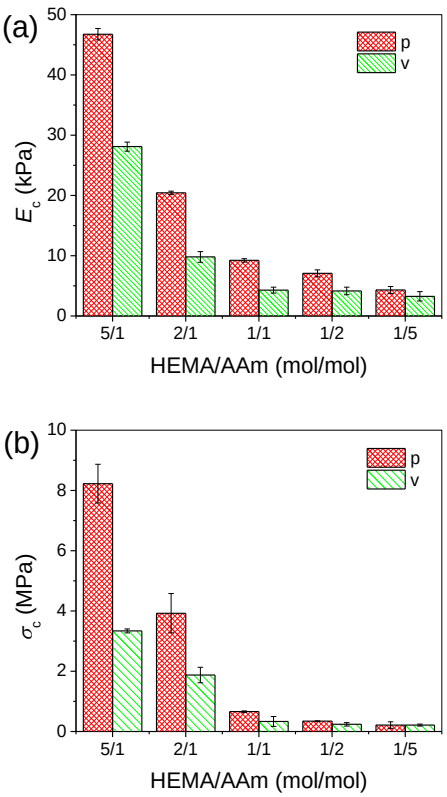

Fig. 6. The moduli (E_c) (a) and compression strengths (σ_c, at ε_c=90%) (b) of the equilibrium swollen P(HEMA-*co*-AAm) hydrogels.

The tensile mechanical properties of the gels were also measured. The typical tensile σ_t-ε_t curves of the gels are shown in Fig. 7a. The gels exhibit moderate tensile mechanical properties. The σ_b′s of the gels are in the range of 25 kPa to 90 kPa, and the ε_b′s are in the range of 2.74-6.00 (mm/mm). The fracture tensile stress (σ_b) and strain (ε_b) of the gels decrease gradually with the increasing molar ratio of AAm.

Interestingly, the gels show almost linear σ_t-ε_t curves (Fig. 7a), especially when the molar ratio of AAm exceeds that of HEMA. The Pearson's r of the σ_t-ε_t curve of Gel-1-1 can reach 0.9999 (Fig. 7b). The linear tensile σ_t-ε_t curve is very exceptional for hydrogels.

Cyclic tensile tests were performed on the gels to the same maximum strains for 5 loading-unloading cycles. For the Gel-5-1, an obvious hysteresis can only be found in the first cycle, but very small hysteresis in the following cycles (Fig. 7c). Whereas for the Gel-1-1, the σ_t-ε_t curves are almost overlapped (Fig. 7d), indicating there is nearly no hysteresis.

The linear relationship between σ_t and ε_t as well as the absence of hysteresis in the loading-unloading cycles suggest that the Gel-1-1 behaves like a spring and hence it might be used as a force or stress sensor.[46, 47]

RSC Advances

RSCPublishing

ARTICLE

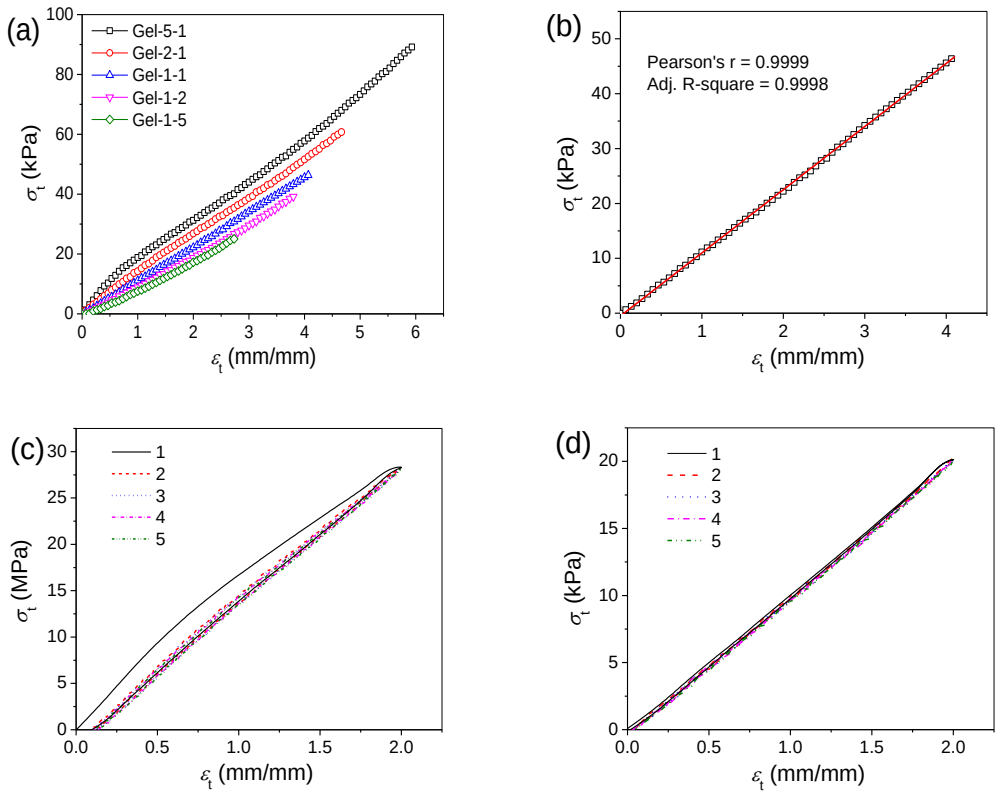

Fig. 7. Tensile properties of the P(HEMA-*co*-AAm) hydrogels. (a): The σ_t-ε_t curves of Gel-x-y in the direction parallel to the freezing direction; (b): the σ_t-ε_t curve of Gel-1-1; and (c, d): the cyclic tensile test curves of Gel-5-1 and Gel-1-1, respectively.

Conclusions

In summary, we demonstrated the fabrication of P(HEMA-*co*-AAm) hydrogels by directional freezing redox polymerization method. Due to the more complicated phase separation induced by using two monomers during the directional freezing process, anisotropic hierarchical porous microstructures are obtained. Very possibly, hydrogels with hierarchical porous structures can also be prepared by using different combinations of monomers. The hydrogels show unidirectional diffusion property and unique water absorbing and losing properties. The hydrogels show anisotropic mechanical properties, with higher elastic moduli and compression strengths in the direction parallel to the freezing direction. Very interestingly, some hydrogels exhibit linear tensile stress-strain curves and extremely low hysteresis in the cyclic loading-unloading curves. We think that the hydrogels may have potential applications as catalyst carriers, substrates for drug delivery and cell culture, bioscaffolds, *etc*.

Acknowledgements

We thank the financial support from the National Science Foundation of China (Nos. 21074014, 21274013) and the Fundamental Research Funds for the Central Universities.

Notes and references

Beijing Key Laboratory of Energy Conversion and Storage Materials, College of Chemistry, Beijing Normal University, Beijing 100875, China. E-mail: wanghl@bnu.edu.cn; Tel: +86 10 58808081; Fax: +86 10 58802075

Electronic Supplementary Information (ESI) available: [Supporting videos showing the water losing of a hydrogel under compression and water absorbing]. See DOI: 10.1039/b000000x/

1. L. E. Lipetz, *Science*, 1961, **133**, 588-593.
2. A. Anssari-Benam, D. L. Bader and H. R. C. Screen, *J. Mater. Sci.: Mater. Med.*, 2011, **22**, 253-262.

3. Z. Fan, J. G. Swadener, J. Y. Rho, M. E. Roy and G. M. Pharr, *J. Orthopaed. Res.*, 2002, **20**, 806-810.
4. J. Zhu, X. Wang, C. He and H. Wang, *J. Mech. Behav. Biomed. Mater.*, 2012, **6**, 63-73.
5. X. Wang, H. Wang and H. R. Brown, *Soft Matter*, 2011, **7**, 211-219.
6. W. Yang, H. Furukawa and J. P. Gong, *Adv. Mater.*, 2008, **20**, 4499-4503.
7. M. A. Haque, T. Kurokawa and J. P. Gong, *Soft Matter*, 2012, **8**, 8008.
8. A. A. Jaeger, C. K. Das, N. Y. Morgan, R. H. Pursley, P. G. McQueen, M. D. Hall, T. J. Pohida and M. M. Gottesman, *Biomaterials*, 2013, **34**, 8301-8313.
9. M. N. Asmani, J. Ai, G. Amoabediny, A. Noroozi, M. Azami, S. Ebrahimi-Barough, M. Navaei-Nigjeh, A. Ai and M. Jafarabadi, *Cell. Biol. Int.*, 2013, **37**, 1340-1349.
10. A. D. Crescenzo, L. Bardini, B. Sinjari, T. Traini, L. Marinelli, M. Carraro, R. Germani, P. Di Profio, S. Caputi, A. Di Stefano, M. Bonchio, F. Paolucci and A. Fontana, *Chemistry*, 2013, **19**, 16415-16423.
11. V. Ramtenki, V. D. Anumon, M. V. Badiger and B. L. V. Prasad, *Colloid. Surface. A.*, 2012, **414**, 296-301.
12. J. H. Ryu, Y. Lee, M. J. Do, S. D. Jo, J. S. Kim, B.-S. Kim, G.-I. Im, T. G. Park and H. Lee, *Acta Biomater.*, 2014, **10**, 224-233.
13. T. Xue, S. Jiang, Y. Qu, Q. Su, R. Cheng, S. Dubin, C.-Y. Chiu, R. Kaner, Y. Huang and X. Duan, *Angew. Chem. Int. Ed.*, 2012, **51**, 3822-3825.
14. C. Chang, N. Peng, M. He, Y. Teramoto, Y. Nishio and L. Zhang, *Carbohyd. Polym.*, 2013, **91**, 7-13.
15. Y. Kosen, H. Miyaji, A. Kato, T. Sugaya and M. Kawanami, *J. Periodontal. Res.*, 2012, **47**, 626-634.
16. U. Schlossmacher, H. C. Schroeder, X. Wang, Q. Feng, B. Diehl-Seifert, S. Neumann, A. Trautwein and W. E. G. Mueller, *RSC Adv.*, 2013, **3**, 11185-11194.
17. J. C. Li and D. C. Dunand, *Acta Mater.*, 2011, **59**, 146-158.
18. R. Zehbe, U. Gross and H. Schubert, in *Bioceramics, Vol 16*, eds. M. A. Barbosa, F. J. Monteiro, R. Correia and B. Leon, 2004, vol. 254-2, pp. 1083-1086.
19. E. P. Gorzkowski and M. J. Pan, *IEEE T. Ultrason. Ferr.*, 2009, **56**, 1613-1616.
20. L. Qian and H. F. Zhang, *J. Chem. Technol. Biotechnol.*, 2011, **86**, 172-184.
21. H. F. Zhang and A. I. Cooper, *Adv. Mater.*, 2007, **19**, 1529-1533.
22. H. F. Zhang, I. Hussain, M. Brust, M. F. Butler, S. P. Rannard and A. I. Cooper, *Nat. Mater.*, 2005, **4**, 787-793.
23. P. M. Hunger, A. E. Donius and U. G. K. Wegst, *J. Mech. Behav. Biomed. Mater.*, 2013, **19**, 87-93.
24. L. Zhang, J. Zhao, J. Zhu, C. He and H. Wang, *Soft Matter*, 2012, **8**, 10439-10447.
25. H. He, D. Zhang and X. Xu, *J. Macromol. Sci. B*, 2012, **51**, 2493-2498.
26. H. E. Romeo, C. E. Hoppe, M. Arturo Lopez-Quintela, R. J. J. Williams, Y. Minaberry and M. Jobbagy, *J. Mater. Chem.*, 2012, **22**, 9195-9201.
27. H. M. Tong, I. Noda and C. C. Gryte, *Colloid Polym. Sci.*, 1984, **262**, 589-595.
28. F. Yokoyama, E. C. Achife, J. Momoda, K. Shimamura and K. Monobe, *Colloid Polym. Sci.*, 1990, **268**, 552-558.
29. M. J. Cooney, C. Lau, M. Windmeisser, B. Y. Liaw, T. Klotzbach and S. D. Minteer, *J. Mater. Chem.*, 2008, **18**, 667-674.
30. X. Qi, J. Ye and Y. Wang, *J. Biomed. Mater. Res. A*, 2009, **89A**, 980-987.
31. N. L. Francis, P. M. Hunger, A. E. Donius, B. W. Riblett, A. Zavaliangos, U. G. K. Wegst and M. A. Wheatley, *J. Biomed. Mater. Res. A*, 2013, **101**, 3493-3503.
32. S. R. Caliari and B. A. C. Harley, *Biomaterials*, 2011, **32**, 5330-5340.
33. X. Wu, Y. Liu, X. Li, P. Wen, Y. Zhang, Y. Long, X. Wang, Y. Guo, F. Xing and J. Gao, *Acta Biomater.*, 2010, **6**, 1167-1177.
34. J. Guan, D. Porter, K. Tian, Z. Shao and X. Chen, *J. Appl. Polym. Sci.*, 2010, **118**, 1658-1665.
35. S. Dogu and O. Okay, *Polymer*, 2008, **49**, 4626-4634.
36. M. Barrow, A. Eltmimi, A. Ahmed, P. Myers and H. Zhang, *J. Mater. Chem.*, 2012, **22**, 11615-11620.
37. M. Barrow and H. Zhang, *Soft Matter*, 2013, **9**, 2723-2729.
38. R. Okaji, K. Taki, S. Nagamine and M. Ohshima, *J. Appl. Polym. Sci.*, 2012, **125**, 2874-2881.
39. M. Chen, J. Zhu, G. Qi, C. He and H. Wang, *Mater. Lett.*, 2012, **89**, 104-107.
40. J. Zhu, J. Wang, Q. Liu, Y. Liu, L. Wang, C. He and H. Wang, *J. Mater. Chem. B*, 2013, **1**, 978-986.
41. J. W. Kim, K. Taki, S. Nagamine and M. Ohshima, *Langmuir*, 2009, **25**, 5304-5312.
42. S. Deville, *Adv. Eng. Mater.*, 2008, **10**, 155-169.
43. S. Deville, E. Maire, A. Lasalle, A. Bogner, C. Gauthier, J. Leloup and C. Guizard, *J. Am. Ceram. Soc.*, 2010, **93**, 2507-2510.
44. S. Deville, E. Saiz, R. K. Nalla and A. P. Tomsia, *Science*, 2006, **311**, 515-518.
45. S. Deville, E. Saiz and A. P. Tomsia, *Acta Mater.*, 2007, **55**, 1965-1974.
46. S. Sulejmani, C. Sonnenfeld, T. Geernaert, G. Luyckx, D. Van Hemelrijck, P. Mergo, W. Urbanczyk, K. Chah, C. Caucheteur, P. Megret, H. Thienpont and F. Berghmans, *Opt. Express*, 2013, **21**, 20404-20416.
47. Y. Yang, D. Q. Yang, H. P. Tian and Y. F. Ji, *Sens. Actuator A*, 2013, **193**, 149-154.